Acceleration-based Control Strategy and Design for Hybrid Electric Vehicle Auxiliary Energy Source

Aree Wangsupphaphol[1], **Nik Rumzi Nik Idris**[2], **Awang Jusoh**[3], **Nik Din Muhamad**[4], and **Supanat Chamchuen**[5], Non-members

ABSTRACT

The paper presents a new control strategy and design for auxiliary energy source (AES) used in battery hybrid electric vehicle (BHEV) based on the acceleration power. The control strategy takes actual speed and acceleration of the vehicle and system losses into account for regulating the energy and power supply to the propulsion load. The design of AES and its dynamic control design are demonstrated. Cascade control is availed in this work in order to control the terminal voltage and current of supercapacitors (SCs). The benefits of AES in which recapture of regenerative braking energy are examined by the numerical simulation and verified by a small scale experiment. The comparison of energy consumption and DC bus voltage regulation between pure battery and battery with supercapacitors (BSCs) propulsion system declares the theoretical results and confirms the benefits of the proposed method.

Keywords: Electric Vehicles, Control Strategy, DC-DC Power Converters, Supercapacitors, Batteries.

1. INTRODUCTION

BEV is the next era of vehicle subsequent the internal combustion engine (ICE) vehicle or hybrid vehicles. Because of the environment problems caused by the ICE and the petroleum fuel absence drive the BEV, zero emission, reborn after disappearing from the commercial trade at the end of 19th century [1]. ICE does not only poor in efficiency but also contributes the global warming by its heat generated, carbons and other hazardous gases. However, the energy per weight of the ICE is lower than the specific energy of batteries; comparing the same power output at the shaft of engine. Moreover, refueling time is much faster than the battery charging period [2].

Manuscript received on September 30, 2014 ; revised on February 1, 2015.

Final manuscript received March 24, 2015.

[1,2,3,4] The authors are with Department of Electrical Power Engineering, Faculty of Electrical Engineering, Universiti Teknologi Malaysia, E-mail: awmr2@live.utm.my, nikrumzi@fke.utm.my, awang@fke.utm.my, nikd@fke.utm.my

[5] The author is with Department of Electrical Engineering, Faculty of Engineering, King Mongkut's University of Technology Thonburi, Thailand, E-mail: ssupanat45b@gmail.com

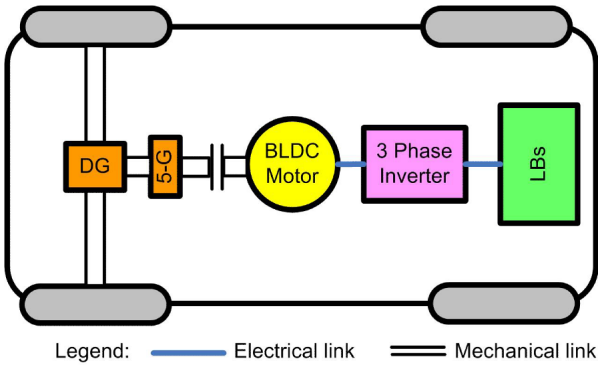

Fig.1: *Configuration of BHEV power train.*

These are significant matters among many designers to overwhelm the problems.

Lithium-ion based battery (LB) is one of an appropriate energy source for BEV. It has higher specific energy and specific power than other batteries; nickel metal hydride, nickel cadmium and lead acid battery. Normally, the particular energy can be up to 265 Wh/kg and the specific power is about 1000 W/kg [3]. The amount of energy states the driving range while the peak power refers to the vehicle acceleration rate.

The acceleration of motor demands the high power and rises the temperature of the battery. This phenomena enlarges the battery internal resistance, on the other hand, it demands great ventilation. Otherwise, the battery can be damaged from overheating. Moreover, to design the battery capacity for peak load requires a large size of battery and absolutely effects to the whole vehicle cost and weight. The improper interfacing of battery with the high acceleration and deceleration causes the low utilization and eventually early failure [4]. Moreover, the battery also has a poor regenerative braking capture capability which reflects the low energy economy. One example is the existing LB using in BEV of this study can absorb about 30 % of the peak power, so the implementation of AES is necessary for energy caption.

Supercapacitor energy storage is one of the best AES assisted to the main energy source proved from its safety concern [5]. The AES can be made of a bank of supercapacitors or an automotive module if

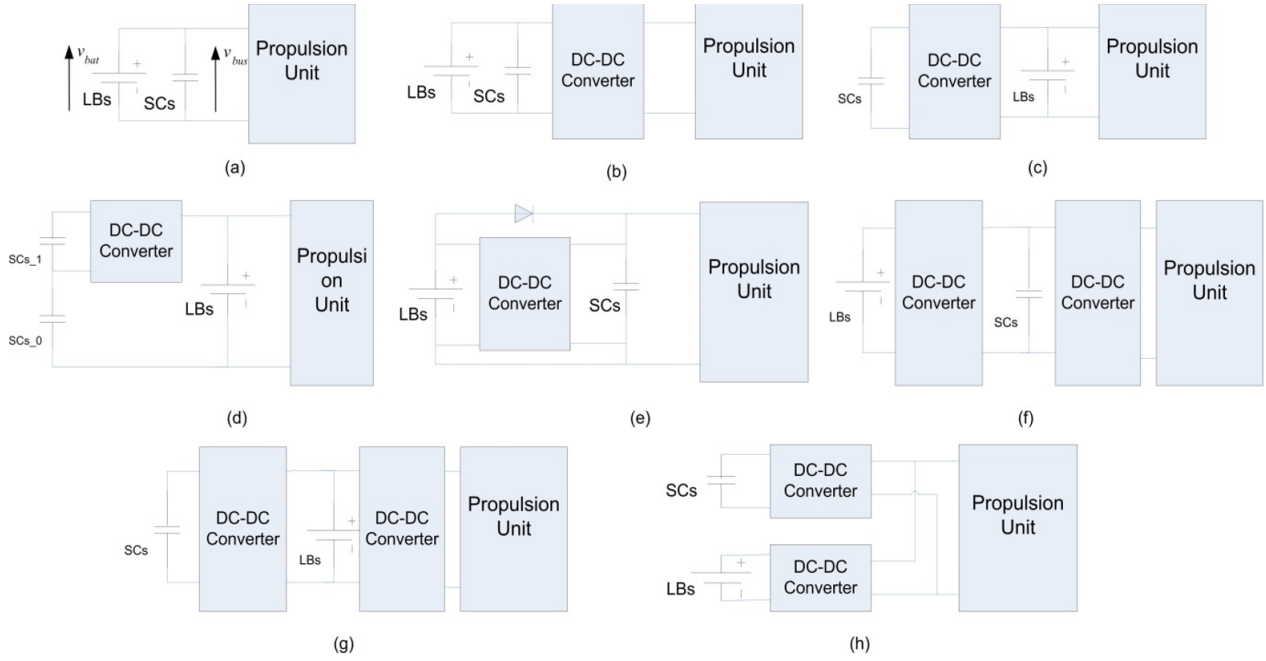

Fig.2: *Possible configurations of hybrid energy source.*

compatible in size. Supercapacitor is an electrochemical double layer capacitor having very high specific area of activated porous carbon for restoring significant amount of capacitance [6]. It has a specific energy around 1-6 Wh/kg while having large amount of specific power about 1-14 kW/kg which is the most compromising solution for a hybrid energy source presently.

There are several possible configurations of hybridizing battery and SCs. Figure 2(a) shows the direct parallel relation between two energy sources supplying the propulsion unit. The terminal voltage of SCs, v_{SCs}, always follows the battery voltage, v_{bat}; where the power flow is proportionally shared depending on their internal resistances. This configuration is easy to implement, but in reality, the SCs stored energy is lowly utilized because its state of charge (SOC) cannot be discharged greatly [4]. Figure 2(b) shows the parallel connection of two energy sources via a converter feeding to propulsion unit. This configuration maintains the bus voltage, v_{bus}, and promotes the inverter efficiency. However, the SCs stored energy is utilized inefficiently because its voltage variation follows the battery voltage, and the converter rated too large for supplying the maximum power [7-8]. The reliability of this hybrid energy source mainly depends on the converter. To control the power of SCs, configuration in Fig. 2(c) is proposed by many researchers for connecting SCs to converter, parallel to the battery, [4], [9-16]. This scheme improves the battery performance by decreasing the battery peak power, reducing loss and rising the temperature. On the other hand, it requires a large size of the converter for providing the peak power. [17-19] introduced configuration as shown in Fig. 2(d) to avoid using large size converter. This scheme separates the SCs into two banks, SCs_0 and SCs_1, and controls only one bank through a controllable converter. Thus, converter rates and losses are lower than the previous scheme, since its active components of the converter are half in size and the inductor is one third smaller. However, the overall terminal of SCs voltage is double the size of the v_{bus}, and it requires a dynamic balancing circuitry, which is expensive and complex. In term of the reliability, configurations in Fig. 2(c) and (d) provide higher reliability than that in Fig. 2(b) even though in the case of converter failure, the vehicle is still available.

By modifying the power sources as shown in Fig. 2(e), the power converter can be minimized [20]. In this case, the battery current supplies average power to the load only when v_{SCs} is higher than v_{bat}, otherwise the battery power can flow through the diode and discharges high power to the load directly. The major disadvantage of this scheme is the large variation of v_{bus} established by the SCs voltage. This behavior concurrently generates high loss of the propulsion inverter. However, this configuration improves the battery performance whenever it is not directly discharged through the diode frequently, and it has equal reliability as the two previous schemes. To overcome the problems of v_{bus} variation, configurations in Fig. 2(f)-(g) have been proposed by some authors [8], [21]. These schemes require a large size converter to provide the dynamic power. Unavoidably, the cost, weight, and loss increase, although they are traded off with the higher efficiency of the propulsion inverter. Besides, their power system reliability is lower than

those in Fig. 2(a) and Fig. 2 (c)-(e); where if one of the converters malfunctions, the vehicle might be inoperative. To control the energy and power of each source completely, multi-converter is implemented, as shown in Fig. 2(h) [22-25]. This configuration presents a steady v_{bus} and protects the battery from high pulsing power demand. Nevertheless, the demerits are similarly found as in the schemes in Fig. 2(f)-(g). In electric vehicle application, the hybrid configuration should be the most reliable, less complex, has low weight, loss and cost. After much consideration, the topology in Fig. 2(c) had been selected to be evaluated in this study, particularly on its dynamic cascade control.

2. SYSTEM CONFIGURATION

2.1 Battery electric vehicle

BEV in this study is basically based on a city saloon vehicle modifying for the electric vehicle challenge [8]. The vehicle has a curb weight of $M_V = 1000$ kg with 2 front-wheel drive. The Differential Gear (DG) and 5-speed Gear (5-G) is simplified for this study to be single gear ratio 1.4288, wheel diameter, $r_{wh} = 0.26$ m, and frontal area $A_f = 2.098$ m^2. The maximum speed is limited at $v_{V,max} = 33.3$ m/s, taking acceleration from 0-100 km/h on the zero degree ground slope around 20 seconds (acceleration rate $a = 1.37$ m/s^2). The traction unit is comprised of a three-phase Brushless DC (BLDC) motor 52 HP, coupled to a three-phase inverter. The drive system has been made simpler by employing a DC motor (DCM) block of SimPowerSystem in MATLAB Simulink, which has the specification as followed: 50 HP, 240 V, maximum angular speed, $\omega_{m,max} = 183.2$ rps, total motor inertia $J_m = 0.2$ kgm^2 and viscous friction coefficient, $B_m = 0.007032$ Nms. The proposed power system is mainly composed of the battery 7.5 V/unit, 32 cells connection in series with the equivalent internal resistance 52 mΩ.

2.2 BHEV hybrid energy source

A hybrid power source is a combination of two or more power sources in order to realize the optimum performance. One of the best solutions is a hybrid between LBs and SCs aforesaid [4]. Nonetheless, there are a number of workable configurations for the hybridization. The selection for application is the most dependable, a few complicated, having low mass, low loss and expenditure. The non-isolate bidirectional DC-DC converter as shown in Fig. 3 was implemented in this work.

2.3 Converter topology for BHEV

The determination of the converter in BHEV is to regulate the dynamic power forward and backward between SCs and tractive load; in a normal case, it works as a boost converter while feeding power and a buck converter when recapturing power. The topology commonly used in an EV is a half bridge non-isolated bi-directional DC-DC converter, as shown in Fig. 3. Among converter topologies, the half bridge converter has more benefits than Cuk and combined SEPIC/Luo converters, which deals high efficiency, being most compact, having bottom cost and less weight and easy to control. The converter requires half size of an inductor and other components compared to the Cuk and combined SEPIC/Luo converters. Switching and conduction losses are lesser, since the lower number of switching components and inductor. However, half bridge converter needs larger size of an output capacitor than other topologies so that keeping continuous output current [26].

2.4 Auxiliary energy source

The AES is made of a bank of SCs connecting to the DC-DC converter. SCs can be a bank of an elementary cell or an automotive module. As regarded, the dynamic power demanded during the acceleration has been considered to be provided by SCs and the tractive power is intended to provide by LBs, so the power from SCs is zero in cruising phase. During braking, SCs is charged to their rated voltage by the dynamic load and LBs power. As renowned, the size of SCs is based on the acceleration power stage; translating mass and the top speed of the BEV are taken into account. In order to evaluate the actual energy availability, the mean efficiencies provided by the manufacturers; SCs, $\boldsymbol{\eta_{SCs}} = 0.95$, converter efficiency, $\boldsymbol{\eta_{conv}} = 0.97$, propulsion chopper efficiency, $\boldsymbol{\eta_{chop}} = 0.97$, DC motor efficiency, $\boldsymbol{\eta_{DCM}} = 0.91$, and mechanical efficiency, $\boldsymbol{\eta_{mech}} = 0.98$, had been taken into consideration. The kinetic energy and energy stored in the SCs were balanced with a definite transformation by losses concurring to the following equation:

$$(M_V + M_{SCs}) v_{V,max}^2 = \eta_{tot} C_{SCs} \left[V_{SCs,max}^2 - \left(\tfrac{1}{2} V_{SCs,max} \right)^2 \right] \tag{1}$$

where $\eta_{tot} = \eta_{SCs} \eta_{conv} \eta_{chop} \eta_{DCM} \eta_{mech}$. SCs terminal voltage is chosen to vary between rated terminal voltage, $V_{SCs,max}$ and half of its rated voltage in order to utilize 75 % of energy content. This produces the optimized capacity and weight of the auxiliary energy source. In order to calculate the SCs capacitance, C_{SCs}, in (1) can be transformed to:

$$C_{SCs} = \frac{(M_V + M_{SCs}) v_{V,max}^2}{\eta_{tot} \left(\frac{3}{4} V_{SCs,max}^2 \right)} \tag{2}$$

The weight of SCs is initially approximated to be zero but subject to change in final calculation. The rated voltage of SCs is selected to achieve the maximum voltage gain lower than 3 [9]. To find the capacitance of a single cell, $C_{SC,cell}$, The C_{SCs} are taken

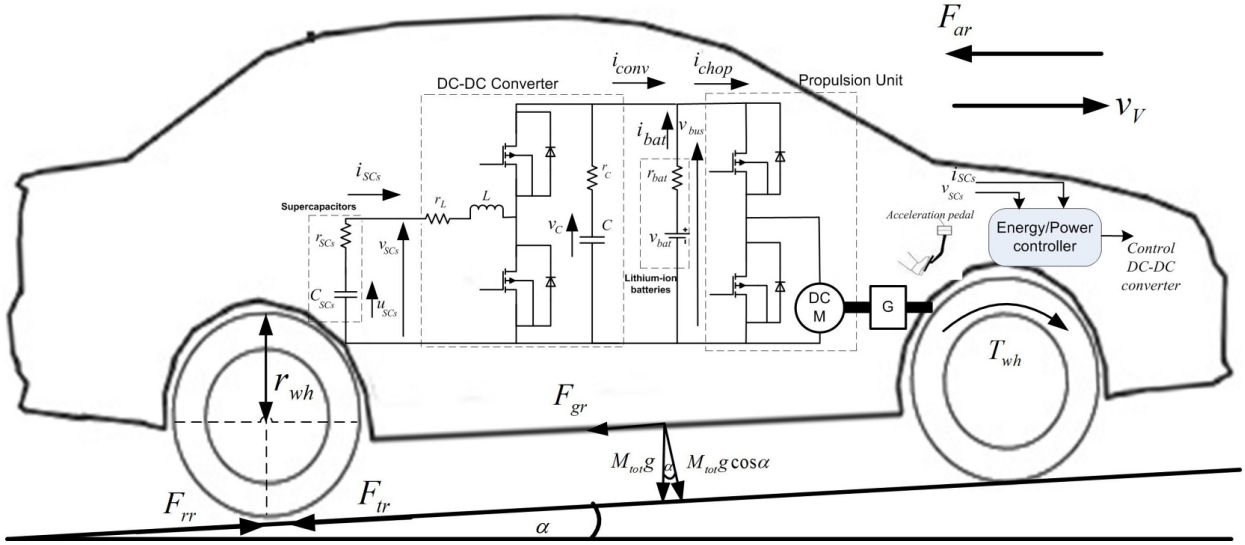

Fig.3: *Power train configuration of the proposed hybrid energy source.*

into account as in the following equation:

$$C_{SCs,cell} = \frac{C_{SCs} \cdot N_s}{N_p} \tag{3}$$

where N_s is the number of series connection and N_p is the number of parallel connection. The N_s can be realized by dividing the SCs terminal voltage with the voltage rating of $C_{SC,cell}$ available. N_p is a selection of an integer number to achieve $C_{SC,cell}$ appropriately to the manufacturer data. In this study, the calculation of C_{SCs} produced 49 Farad, where SCs terminal rated voltage of 200 V was chosen. This was made by a parallel connection of series $C_{SC,cell}$ = 2000 Farad, 74 cells, 2.7 V/cell. However, the connection produced C_{SCs} = 54 Farad with internal resistance 26 mΩ and 53 kg. These increased the capacitance by 10% and weight by 5%. The capacitance and weight were final calculated to ensure the vehicle performance and found that it was maintained.

To evaluate the rated power of SCs in acceleration, $P_{SCs,acc}$, maximum acceleration rate a=1.37 ms$^(-2)$ was implemented to design the converter capacity as the following equation:

$$P_{SCs,acc} = \frac{M_{tot} v_{V,max} a}{\eta_{conv}\eta_{chop}\eta_{DCM}\eta_{mech}} = 57.1 \text{ kW} \tag{4}$$

where $M_{tot} = M_V + M_{SCs}$ is the total vehicle mass. After that, the current was evaluated by using the following equation:

$$I_{SCs,acc} = \frac{P_{SCs,acc}}{V_{SCs,max}/2} = 571 \text{ A} \tag{5}$$

where $I_{SCs,acc}$ is accelerated current of SCs. From the calculation, the current of each series distributes by 286 A which is endorsed by the maximum peak current of 1600 A, according to manufacturer specification.

3. MATHEMATICAL MODEL OF THE PHYSICAL SYSTEM

3.1 Model of propulsion load

Power demanded by the propulsion chopper, P_{chop}, can be developed mathematically as the following equations:

$$P_{chop} = \begin{cases} P_d/\eta_{chop}\eta_{DCM}; & P_d > 0 \\ P_d\eta_{chop}\eta_{DCM}; & P_d < 0 \end{cases} \tag{6}$$

$$P_d = P_{tl} + P_{dl} \tag{7}$$

where P_d is the driving power, P_{tl} is the tractive load power and P_{dl} is the dynamic load power at motor shaft. To obtain the tractive load power, vehicle dynamic resistances have to be derived by using (8), where F_{tr} is the tractive resistance, F_{rr} is the rolling resistance generated between tires and road surfaces, F_{ar} is aerodynamic resistance dragging the vehicle motion to move into the air, F_{gr} is the grading resistance that downgrades the force of vehicle, T_{wh} is the load torque at wheel, T_{eq} is the equivalent load torque transferred through the single gear ratio G.

$$\begin{cases} F_{tr} = F_{rr} + F_{ar} + F_{gr} \\ F_{rr} = \mu_{rr} M_{tot} g \cos\alpha \\ F_{ar} = 0.5\rho A_f C_d v_{V,max}^2 \\ F_{gr} = M_{tot} g \sin\alpha \\ T_{wh} = F_{tr} r_{wh}; T_{eq} = T_{wh}\eta_{mech}/G \\ G = \omega_{m,max}/\omega_{wh,max} \\ P_{tl} = T_{eq}\omega_{m,max} = 18.38 \text{ kW} \end{cases} \quad (8)$$

Any coefficient values for calculation were as follows: rolling resistance μ_{rr} =0.0048, Air density ρ = 1.25 kgm^{-3}, aerodynamic drag C_d = 0.353, gravity acceleration rate g = 9.8 ms^{-2}, and road grading angle α = 0 degree. The dynamic power, P_{dl}, was reacted by SCs, which diverse to the angular acceleration rate of the propulsion load, according to the following equations:

$$\begin{cases} P_{dl} = T_{dl}\omega_{m.max} = 48 \text{ kW} \\ T_{dl} = J_{eq}\frac{d\omega_m}{d_t} = 262 \text{ N}\cdot\text{m} \\ J_{eq} = J_m + M_{tot}\eta_{mech}\left(\frac{r_{wh}}{G}\right)^2 = 34.2 \text{ kg}\cdot\text{m}^{-2} \end{cases} \quad (9)$$

where T_{dl} is the dynamic load torque, J_{eq} is the equivalent moment of inertia referred to the motor shaft. By solving the equation, P_{dl} = 48.31 kW, the SCs size for the acceleration power can be approximated by:

$$P_{SCs,acc} = P_{dl}/\eta_{conv}\eta_{chop}\eta_{DCM} = 56.1\text{kW} \quad (10)$$

3.2 Model of auxiliary energy source and battery system

The equivalent circuit of SCs can be modeled as the *RC* series circuit as shown in Fig. 3. The equivalent electric circuit model is evaluated by the following equations:

$$\begin{cases} i_{SCs}(t) = -C_{SCs}\frac{du_{SCs}}{dt} \\ V_{SCs}(t) = u_{SCs} - r_{SCs}i_{SCs} \\ u_{SCs}(0) = V_{SCs,max} \end{cases} \quad (11)$$

where u_{SCs} is the internal voltage of SCs, r_{SCs} is the internal resistance of SCs and v_{SCs} is the terminal voltage of SCs and i_{SCs} is SCs current .

In application, bus voltage, v_{bus}, varies to the internal battery voltage, v_{bat}, and the battery current, i_{bat}. The bus voltage is changed by SOC and the voltage drop across the equivalent battery resistance, r_{bat}, as in the following equations:

$$\begin{cases} v_{bat} \propto SOC \\ v_{bus} = v_{bat} - r_{bat}i_{bat} \end{cases} \quad (12)$$

4. CONTROL STRATEGY AND DESIGN

4.1 Control strategy

The main objective of the control strategy is to reduce pulse discharge of the battery and recapture much more regenerative energy. The energy conservation perspective has been implemented in this study. In order to manage the energy, the auxiliary energy source terminal voltage is varied to the speed of vehicle or, on the other hand, the kinetic energy, as in the following equation:

$$u_{SCs,ref} \cong \sqrt{V_{SCs,max}^2 - \frac{M_{tot}v_{ref}^2}{\eta_{tot}C_{SCs}}} \quad (13)$$

With the purpose of power control, SCs current and voltage are controlled simultaneously. The fundamental relation in (11) is availed to control the current by replacing with (13). This results in reference current control relating to the speed and acceleration of the vehicle as shown in the following equation:

$$i_{SCs,ref} = -C_{SCs}\frac{du_{SCs,ref}}{dt} \cong \frac{\frac{M_{tot}v_{V,ref}}{\eta_{tot}V_{SCs,max}}}{\sqrt{1-\frac{M_{tot}v_{V,ref}^2}{\eta_{tot}C_{SCs}v_{SCs,max}^2}}}\frac{dv_{V,ref}}{dt} \quad (14)$$

Similarly, the strategy provided the ability to supply and capture power according to the acceleration or deceleration and the conversion of energies between the two storages.

4.2 Converter design

Cascade control is utilized to control the driving power by regulating duty cycle current of the inner loop received from the outer voltage control loop. To control the outer and inner loop, the linearization of converters state equation has to be derived by using state space averaging technique. The system matrices, $A_{1,2}, B_{1,2}$ and $C_{1,2}$, can be achieved by using KVL in the on and off stage of the boost converter [7] as shown in the following equations:

$$\begin{cases} A_1 = \begin{bmatrix} \frac{-(r_L + r_{SCs})}{L} & 0 \\ 0 & -\frac{1}{C(R+r_C)} \end{bmatrix}, B_1 = \begin{bmatrix} \frac{1}{L} \\ 0 \end{bmatrix}, C_1 = [1 \quad 0] \\ \quad ; \text{system matrices during on stage} \\ A_2 = \begin{bmatrix} \frac{-(R_{rc} + R(r_L + r_{SCs}))}{L(R+r_C)} & \frac{-R}{L(R+r_C)} \\ \frac{R}{C(R+r_C)} & \frac{-1}{C(R+r_C)} \end{bmatrix}, B_2 = \begin{bmatrix} \frac{1}{L} \\ 0 \end{bmatrix}, C_2 = [1 \quad 0] \\ \quad ; \text{system matrices during off stage} \end{cases} \quad (15)$$

where R is the equivalent resistance of maximum power supply by SCs, 2.1 Ω, L is the converter inductance 0.1 mH, r_L is the equivalent inductive resistance 20 mΩ, C is the converter capacitance 10 mF and r_C is the equivalent capacitive resistance 25 mΩ. Equation (16) presents the system matrices of on and off interval, which are used for linearizing the system

at the quiescent operating point. To obtain the transfer function of duty ratio, D, to the SCs current, the state equation can be settled by the following equation:

$$\frac{I_{SCs}(s)}{D(s)} = C_s(sl - A_s)^{-1}[(A_1 - A_2)X + (B_1 - B_2)U] + (C_1 - C_2)X \quad (16)$$

where X is the equilibrium state vector and U is the equilibrium input vector. Equation (16) can be transformed to the standard equation of MATLAB transient response analysis for finding the transfer function as following:

$$\frac{I_{SCs}(s)}{D(s)} = C_s(sl - A_s)^{-1}B_s + E_s \quad (17)$$

where A_s, B_s, C_s and E_s are the group of matrix as described by the following equations:

$$\begin{cases} A_s = A_1 D + A_2(1 - D) \\ B_2 = (A_1 - A_2)X + (B_1 - B_2)U \\ C_s = C_1 D + C_2(1 - D) \\ E_s = (C_1 - C_2)X \end{cases} \quad (18)$$

Thereby, the duty ratio to inductor current can be derived. The outer loop, SCs current to SCs voltage, is the pure integrator of inversion of capacitance. Subsequently, the PI controller of MATLAB/Simulink is implemented and tuned for the stability as shown in Fig. 4.

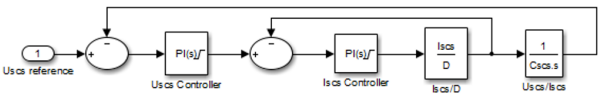

Fig.4: *Cascade control for SCs.*

After receiving the proper PI controllers, they have been simulated with the real scale parameter of the BHEV as shown in Fig. 5 in order to observe the behavior of the proposed system.

5. TEST BENCH AND SIMULATION RESULTS

5.1 Test bench

The electromechanical hardware as shown in Fig. 6 consists of rechargeable lead-acid batteries, SCs, DC motor with flywheel and dSPACE controller card DS1104 was set up for the simulation and experiment. The energy sources were the hybridized between batteries 12 V/cell connected in series for 7 units and SC 25 F, 2.7 V/cell connected in series for 30 units through a controllable bidirectional dc-dc converter. The separated field excite DC motor connected with

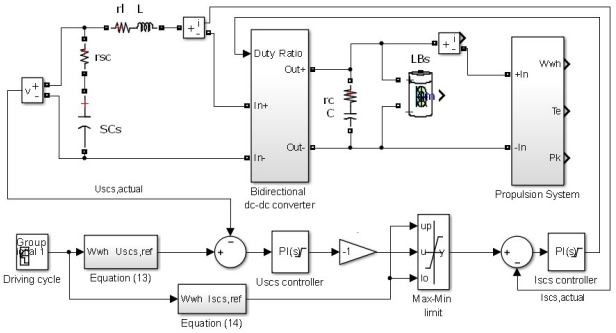

Fig.5: *MATLAB/Simulink block diagram for the BHEV power train system.*

flywheels were used as the active load. The parameters of the hardware are shown in Table 1.

5.2 Simulation results

The small-scale experiment was simulated in order to validate the proposed control technique by using

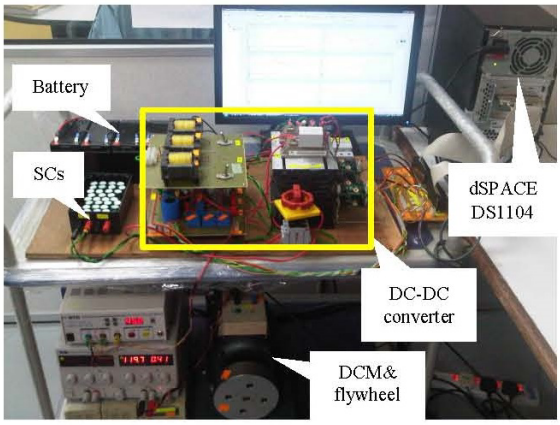

Fig.6: *Front view of the experimental hardware.*

Table 1: *Experimental Hardware Parameters.*

Lead-acid battery		
Rated/Floating voltage	[V]	12/13.5
Maximum discharge/charge	[A]	105/2.1
Capacity	[Ah]	7
Internal resistance	[mΩ]	23
Supercapacitor		
Rated voltage	[V]	2.7
Capacitance	[F]	25
Internal resistance	[mΩ]	25
Bidirectional dc-dc converter		
Inductor/ESR	[mH/mΩ]	5/500
Output capacitor/ESR	[mF/mΩ]	10/25
IGBT modules	Fuji	2MBI100TA-060
DC motor and load		
Rate voltage/current	[V/A]	120/3.3
Rated power	[W]	250
Rated speed	[rpm]	3000
Weight/inertial (with flywheel)	[kg/kgm^2]	14/0.03

numerical simulation. The simulation is not only for preliminary observation but also for safety reason before the experiment, so the switching model of 20 kHz as same as in experiment was used as the same in experiment.

The maximum acceleration driving cycle, which is composed of the acceleration, cruising and braking, was supplied to the controller of SCs to generate the reference voltage and current. According to the driving cycle, the motor was started at t = 6 s and sprinted up to the maximum speed of 183 rps at t = 13 s, after that the motor speed was maintained for 5 s and decelerated until stoppage from t = 18-25 s as shown in Fig. 7(a) where the reference and actual speed were completely superimposed. Power sharing diagram can be observed in Fig. 7(b) where battery provided a small amount of power in acceleration, while SCs supplied larger amount of 200 W for the motor acceleration. In cruising phase, the battery responded for the tractive power alone at 60 W while SCs was silent. At the starting of braking phase, the battery supplied high peak power of 150 W together with the regenerative braking power 100 W to charge SCs. DC bus voltage of pure battery and BSCs experiments were compared to observe the effectiveness of the proposed

technique. They can be observed in Fig. 7(c), where voltage regulation of 0.5% and 0.34% were provide by the pure battery and BSCs respectively, and these clearly show that the proposed technique reduces the battery voltage varying in propulsion application.

Energy consumption comparison for the driving cycle between pure battery and BSCs is reported in Fig. 7(d) where the end of cycle, BSCs and pure battery consumed 0.285 W and 0.305 W respectively, and this can be considered that the energy was saved 6

6. EXPERIMENTAL RESULTS

The electromechanical experiment is used for verifying the simulation results presented previously. The agreement of the experimental results along with the simulation as aforesaid is shown as in Fig. 8(a)-(d). In Fig. 8(a), the actual speed is completely overlaid the reference speed that accelerating from t = 6-13 s to the motor speed of 183 rps, cruising for 5 s, and braking between t = 18 - 25 s, as same in the simulation. Power sharing between the battery and SCs is shown in Fig. 8(b). At t = 2 s, the battery was connected to the power system, so it can be seen that the transient battery power was pre-charged to output capacitor of bidirectional converter. At t = 6 s, the motor was accelerated where the battery provided a little amount of power at the early stage, but it was inserted by the inclining SCs power till it was zero at the end of acceleration phase. The SCs supplied power until reaching the maximum at 180 W,

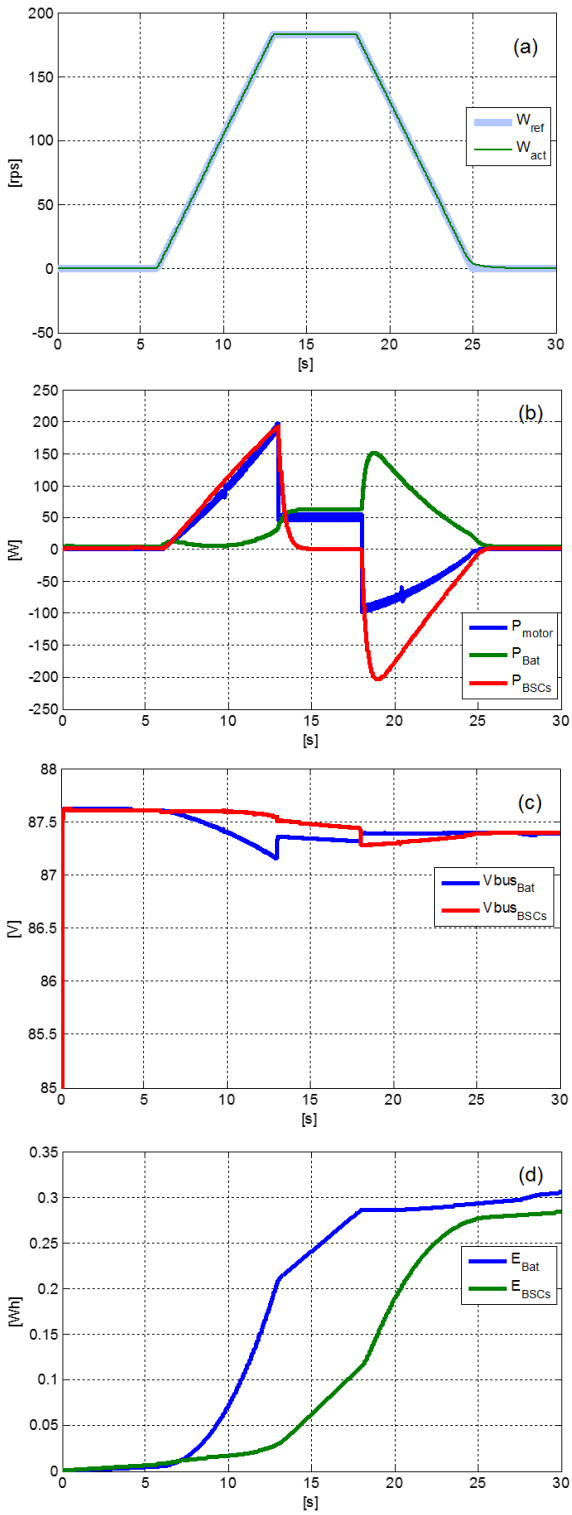

Fig.7: *Simulation results: (a) reference and actual speed (b) batteries, SCs, and motor output power, (c) DC bus voltage of pure battery and BSCs, and (d) energy consumption of pure battery and BSCs.*

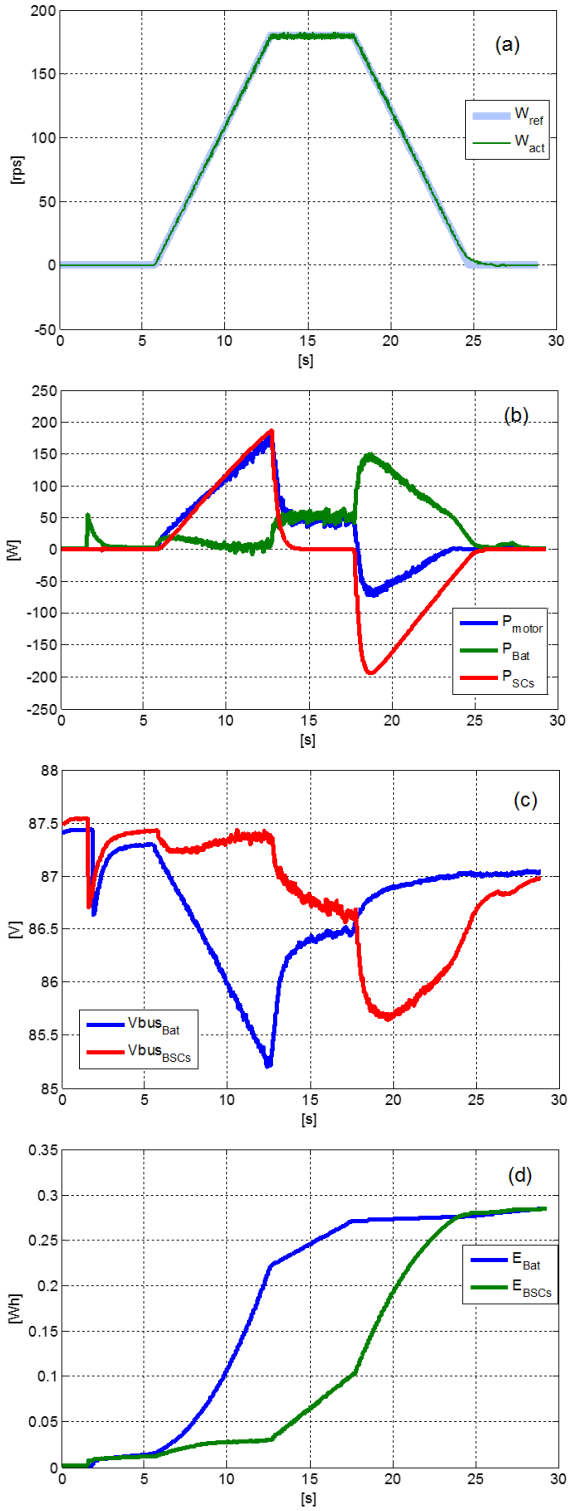

Fig.8: *Experimental results: (a) reference and actual speed (b) batteries, SCs, and motor output power, (c) DC bus voltage of pure battery and BSCs, and (d) energy consumption of pure battery and BSCs.*

and it was zero in cruising phase at t = 13 s where the battery fed tractive power 60 W until the end of this phase. In braking phase starting at t = 18 s, the motor acted as a generator supplying power 70 W to the SCs with the battery power 150 W for charging the SCs fully. The SCs charging losses in any components can be observed from the power summation in this stage, and it has the same behavior as in the simulation. This clearly shows that the result in Fig. 8(b) accompanies with the result in simulation. Fig. 8(c) shows the comparison of DC bus voltage regulation between the pure battery and BSCs where they are 2.5% and 2.17% respectively, so the advantage of BSCs is the decrease of voltage regulation by 0.33%. Energy consumption for the driving cycle was presented in Fig. 8(d) where the BSCs consume almost the same as pure battery. This because the tolerance and non-linearity of the hardware, so the profit in term of energy consumption was not achieved.

7. CONCLUSIONS AND FUTURE WORK

This paper presents a new control strategy and a reliable DC-DC converter for SCs auxiliary energy source using in BHEV, fore reducing the energy consumption of the battery and improve the DC voltage regulation. The proposed strategy is to control SOC and current of SCs according to the speed and acceleration of the vehicle. The simulation successfully proved the benefits of the BSCs over the pure battery by saving energy of 6% and reducing of DC bus voltage regulation by 0.16%. The experimental results verify the workability of the control strategy where the proposed system reduced voltage regulation by 0.33%. However, the energy consumption between pure battery and BSCs in the experiment showed the same amount at the end of driving cycle tested. This can be improved by the further optimization the real system for a specific application.

ACKNOWLEDGEMENT

The author would like to thanks for finance supported by the PhD. Merit Scholarship of Islamic Development Bank (IDB) for conducting the research at UTM-Proton future drive.

References

[1] M. Ehsani, Y. Gao, and A. Emadi, *Modern electric, hybrid electric*, and fuel cell vehicles: fundamentals, theory, and design. CRC press, 2009, pp. 13-15.

[2] L. James and L. John, *Electric Vehicle Technology Explained*, John Wiley and Sons, Inc., New York, 2003, pp. 1-5.

[3] Lithium-ion battery. Available http://en.wikipedia.org/wiki/Lithium-ion_battery

[4] S. Pay and Y. Baghzouz, "Effectiveness of battery-supercapacitor combination in electric vehicles," in *Power Tech Conference Proceedings, 2003 IEEE Bologna*, 2003, vol. 3, pp. 1-6.

[5] G. Zorpette, "Super charged," *Spectrum, IEEE*, vol. 42, No. 1, 2005, pp. 32-37.

[6] M. Steiner, M. Klohr, and S. Pagiela, "Energy storage system with ultracaps on board of railway vehicles," in *Power Electronics and Applications*, 2007 European Conference on, 2007, pp. 1-10.

[7] S. M. Lukic, S. G. Wirasingha, F. Rodriguez, J. Cao, and A. Emadi, "Power management of an ultracapacitor/battery hybrid energy storage system in an hev," in *Vehicle Power and Propulsion Conference*, 2006. VPPC'06. IEEE, 2006, pp. 1-6.

[8] I. Aharon and A. Kuperman, "Topological overview of powertrains for battery-powered vehicles with range extenders," *Power Electronics, IEEE Transactions on*, vol. 26, No. 3, pp. 868-876, 2011.

[9] D. Iannuzzi and P. Tricoli, "Speed-based state-of-charge tracking control for metro trains with onboard supercapacitors," *Power Electronics, IEEE Transactions on*, vol. 27, No. 4, pp. 2129-2140, 2012.

[10] M. Ortzar, J. Moreno, and J. Dixon, "Ultracapacitor-based auxiliary energy system for an electric vehicle: Implementation and evaluation," *Industrial Electronics, IEEE Transactions on*, vol. 54, No. 4, pp. 2147-2156, 2007.

[11] N. JInrui, S. Fengchun, and R. Qinglian, "A study of energy management system of electric vehicles," in *Vehicle Power and Propulsion Conference*, 2006. VPPC'06. IEEE, 2006, pp. 1-6.

[12] A. Jarushi and N. Schofield, "Battery and supercapacitor combination for a series hybrid electric vehicle," in *Power Electronics, Machines and Drives (PEMD 2010), 5th IET International Conference on*, 2010, pp. 1-6.

[13] M. Ortuzar, J. Dixon, and J. Moreno, "Design, construction and performance of a buck-boost converter for an ultracapacitor-based auxiliary energy system for electric vehicles," in *Industrial Electronics Society, 2003. IECON'03. The 29th Annual Conference of the IEEE*, 2003, vol. 3, pp. 2889-2894.

[14] B. Arnet and L. Haines, "High power DC-to-DC converter for supercapacitors," in *Electric Machines and Drives Conference, 2001. IEMDC 2001. IEEE International*, 2001, pp. 985-990.

[15] L. Gao, R. A. Dougal, and S. Liu, "Power enhancement of an actively controlled battery/ultracapacitor hybrid," *Power Electronics, IEEE Transactions on*, vol. 20, No. 1, pp. 236-243, 2005.

[16] J. W. Dixon, M. Ortzar, and E. Wiechmann, "Regenerative braking for an electric vehicle using ultracapacitors and a buck-boost converter," in *17th Electric Vehicle Symposium (EVS17)*,(Canada), 2000, pp. 1-11.

[17] G. Guidi, T. Undeland, and Y. Hori, "An optimized converter for battery-supercapacitor interface," in *Power Electronics Specialists Conference*, 2007. PESC 2007. IEEE, 2007, pp. 2976-2981.

[18] G. Guidi, T. M. Undeland, and Y. Hon, "An interface converter with reduced VA ratings for battery-supercapacitor mixed systems," in *Power Conversion Conference-Nagoya*, 2007. PCC'07, 2007, pp. 936-941.

[19] G. Samson, T. M. Undeland, O. Ulleberg, and P. Vie, "Optimal load sharing strategy in a hybrid power system based on pv/fuel cell/battery/supercapacitor," in *Clean Electrical Power, 2009 International Conference on*, 2009, pp. 141-146.

[20] J. Cao and A. Emadi, "A new battery/ultracapacitor hybrid energy storage system for electric, hybrid, and plug-in hybrid electric vehicles," *Power Electronics, IEEE Transactions on*, vol. 27, No. 1, pp. 122-132, 2012.

[21] S. F. Tie and C. W. Tan, "A review of energy sources and energy management system in electric vehicles," *Renewable and Sustainable Energy Reviews*, vol. 20, pp. 82-102, 2013.

[22] J. Wong, N. Idris, M. Anwari, and T. Taufik, "A parallel energy-sharing control for fuel cell-battery-ultracapacitor hybrid vehicle," in *Energy Conversion Congress and Exposition (ECCE)*, 2011 IEEE, 2011, pp. 2923-2929.

[23] L. Solero, A. Lidozzi, and J. A. Pomilio, "Design of multiple-input power converter for hybrid vehicles," *Power Electronics, IEEE Transactions on*, vol. 20, No. 5, pp. 1007-1016, 2005.

[24] A. Florescu, H. Turker, S. Bacha, and E. Vinot, "Energy management system for hybrid electric vehicle: Real-time validation of the VEHLIB dedicated library," in *Vehicle Power and Propulsion Conference (VPPC)*, 2011 IEEE, 2011, pp. 1-6.

[25] M. Jain, C. Desai, and S. S. Williamson, "Genetic algorithm based optimal powertrain component sizing and control strategy design for a fuel cell hybrid electric bus," in *Vehicle Power and Propulsion Conference*, 2009. VPPC'09. IEEE, 2009, pp. 980-985.

[26] R. M. Schupbach and J. C. Balda, "Comparing DC-DC converters for power management in hybrid electric vehicles," in *Electric Machines and Drives Conference, 2003. IEMDC'03. IEEE International*, 2003, vol. 3, pp. 1369-1374.

Aree Wangsupphaphol was born in Bangkok, Thailand, in 1975. He received B.Eng. and M.Eng. degrees in electrical engineering from King Mongkut's Institute of Technology Ladkrabang, Thailand, in 1999 and 2007 respectively. He becomes a Special Lecturer in the Rail Transportation Engineering, Department of Mechanical Engineering, King Mongkut's Institute of Technology Ladkrabang in 2014. His research interests include energy management system, electric vehicle applications, and control of power electronics systems.

Nik Rumzi Nik Idris received the B.Eng. degree in electrical engineering from the University of Wollongong, Australia, in 1989, the M.Sc. degree in power electronics from Bradford University, West Yorkshire, U.K., in 1993, and the Ph.D. degree from Universiti Teknologi Malaysia, Malaysia, in 2000. He is an Associate Professor at the Faculty of Electrical Engineering, Universiti Teknologi Malaysia. His research interests include ac drive systems and DSP applications in power electronic systems. Dr. Idris is a senior member of the IEEE and the Chair for the Power Electronics Chapter of the IEEE Malaysia Section for 2014-2015.

Awang Jusoh was born in Terengganu, Malaysia in 1964. He received his B.Eng. degree from Brighton Polytechnic, U.K., in 1988. He obtained his M.Sc. and Ph.D. degrees from the University of Birmingham, U.K., in 1995 and 2004, respectively. He is currently with the Department of Power Engineering, Faculty of Electrical Engineering, Universiti Teknologi Malaysia, Malaysia. His research interests are in DC-DC converter, renewable energy, and control of power electronics systems.

Nik Din Muhamad received B.Eng. (Hons.) and M.Eng. degrees in electrical engineering from Universiti Teknologi Malaysia, Malaysia, in 1988 and 1999 respectively. He is currently a senior lecturer with Universiti Teknologi Malaysia, Malaysia. His research interests include modeling and control of power electronic systems.

Supanat Chamchuen was born in Kalasin, Thailand, in 1992. He is studying B.Eng. degree in electrical engineering at King Mongkut's University of Technology Thonburi, Thailand. He was an internship student at the UTM-PROTON Future Drives Laboratory, Universiti Teknologi Malaysia, Malaysia during June-July 2014. His research interests are in electric motor drives and railway electrification.